Preparation and characterization of 2D SiC/SiC composites with composition-graded C(B) interphase

Sylvain Jacques, A. Guette, F. Langlais, R. Naslain, S. Goujard

PREPARATION AND CHARACTERIZATION OF 2D SiC/SiC COMPOSITES WITH COMPOSITION GRADED C(B) INTERPHASE

S. JACQUES, A. GUETTE, F. LANGLAIS and R. NASLAIN

Laboratoire des Composites Thermostructuraux

UMR 47 CNRS–SEP–UB1, Université Bordeaux-I

3, allée de la Boëtie, 33600 Pessac, France

S. GOUJARD

Société Européenne de Propulsion

BP 37, 33165 Saint Médard-en-Jalles, France

ABSTRACT

2D SiC/C(B)/SiC composites were prepared by CVI. The C(B) interphase, deposited by CVI from the $C_3H_8/BCl_3/H_2$ gaseous precursor, is made of five successive C(B)-layers with increasing boron content from the fiber to the matrix. This composition graded interphase permits to achieve good mechanical properties similar to those obtained with pure pyrocarbon interphase. But, surprisingly, the lifetime in air under load at high temperature of 2D SiC/C(B)/SiC composites is not improved despite the high percentage of boron in several sublayers of the interphase. These behaviors has been explained through TEM characterization of the interphase before and after matrix infiltration as well as after thermal ageing. The layer containing a low boron content (about 8 at. %) is highly organized with carbon planes parallel to the fiber axis, a feature which favors the crack deflections. Conversely, the boron-rich layers exhibit a nano-porous texture probably due to a bad control of the growth process within the fibrous preforms. This nano-porous texture might be responsible for the poor oxidation resistance of these

sublayers and consequently the rather short lifetime of the real 2D composites with respect to those previously reported for 1D SiC/C(B)/SiC model microcomposites.

KEY WORDS

SiC/SiC COMPOSITES, STRUCTURE, TEM, C(B) INTERPHASE, GRADIENT COMPOSITION INTERPHASE, LIFETIME UNDER LOAD, OXIDATION, TENSILE BEHAVIOR

1. Introduction

Turbostratic pyrolytic carbon is a classical interphase material in the 2D SiC/SiC composites, owing to its ability to deflect the cracks originating in the matrix and to protect the fiber from damaging [1-3]. In a recent study on SiC/SiC microcomposites, the addition of boron in pyrocarbon interphase (up to 33 at. %) has been shown to improve the oxidation resistance of these materials but to decrease their mechanical characteristics. By using a composition graded C(B) interphase, with a boron content increasing from 0 near the fiber to 33 at. % near the matrix, microcomposites were obtained with both good mechanical properties and high oxidation resistance [4].

The present paper deals with the preparation and characterization of this kind of interphase within actual 2D SiC/SiC composites.

2. Experimental

Stacks of 10 fabrics of 2D woven fibers[1] maintained pressed together with a graphite tooling were chemical vapor infiltrated (CVI) with a composition graded C(B) interphase (Fig. 1). The synthesis conditions were similar to those used in the previous study carried out on microcomposites [4]. The boron content of this interphase was increasing from 0 at. % B near the fiber to 33 at. % B near the matrix. The gaseous precursor was a $C_3H_8/BCl_3/H_2$ mixture and the graded composition of the deposit resulted from a step variation of the initial gas phase ratio $\alpha = 100 \times Q(BCl_3) / [Q(C_3H_8) + Q(BCl_3)]$ where Q(i) is the partial flow rate of species i. The infiltration durations were selected in order to obtain layers with constant thicknesses and a total interphase thickness of about 0.4 μm (Table 1). The total pressure and temperature of the CVI process were respectively 1.0 kPa and 950 °C. After the interphase deposition, some fibers were extracted from the preform and characterized by Auger electron spectrometry (AES)[2] in order to control the boron concentration gradient.

Finally, the 2D SiC/SiC composites were obtained by CVI of silicon carbide (SiC being the matrix) from a CH_3SiCl_3 (MTS)/H_2 precursor, according to a process which has been described elsewhere [5].

Three tensile specimens 8.5 cm in length were machined from these composites and were tensile tested at ambient temperature (with loading-unloading cycles in one test). The tensile stress was calculated from the applied load, assuming that the variations of the specimen cross-section area during loading could be neglected. The tensile strain was measured with an extensometer with a 25 mm gauge length. Six other test samples (0.33 x 1 x 6 cm^3) were submitted to air ageing treatment at high temperature and under a constant load in four points bending corresponding to a stress of 150 MPa. Two samples were tested at 500 °C, two at 600 °C and two at 700 °C.

Three types of samples were characterized by transmission electron microscopy

---

[1] Si-C-O NICALON fiber (ceramic grade, NLM 202) from Nippon Carbon, Japan.

[2] PHI 590 SAM from Physical Electronics / Perkin Elmer.

(TEM)[3]. The first was taken from a sample which has been submitted to the ambient tensile test with load cycles (Fig. 2.a). The second was taken from a specimen which has been aged under a four points bending load corresponding to a stress of 150 MPa at 600 °C (Fig. 2.b) and the third was made of fibers extracted from a 2D preform only infiltrated with the C(B) composition graded interphase. Thin foils were prepared for the two first samples according to a classical procedure, i.e. the composite was embedded in an epoxy resin, the interesting parts were cut off with a diamond wire saw, thinned by mechanical polishing and then ion milling[4]. For the third sample, a specific procedure already described for the microcomposites study, was used [6]. The C(B) interphases were observed in TEM using bright field and high resolution techniques. For symmetrical C-002 lattice imaging, a 11.5 nm^{-1} objective opening was used. The interphase composition was locally analysed by electron energy loss spectroscopy (EELS)[5] with a probe diameter of about 20 nm.

3. Results and discussion

3.1. AES interphase characterization

Figure 3 gives the atomic concentration profiles within the interphase measured by AES in-depth and near the external surface of 2D SiC/C(B)/SiC composites preforms. Carbon and boron contents are similar to those obtained previously in SiC/C(B)/SiC microcomposites [4]. Conversely, the infiltration leads to different thicknesses of this interphase between the center and the periphery of the 2D preform (respectively ≈ 400 nm and ≈ 800 nm, reference: Ta_2O_5).

---

[3] CM 30 ST from PHILIPS, The Netherlands.
[4] 600 Duo Mill from GATAN, USA.
[5] Gatan.

3.2. Ambient tensile tests.

The strain and stress to failure of SiC/C(B)/SiC 2D composites measured through three tensile tests were 0.96 % and 330 MPa, 1.1 % and 340 MPa and 1.1 % and 350 MPa. The proportional limit was about 65 MPa. These values are very close to those obtained for the classical pyrocarbon interphase in SiC/PyC/SiC composites [7], as previously reported for microcomposites [4]. Figure 4 shows the tensile tests curves with loading-unloading cycles for both types of 2D composites. Both behaviors are very similar. The hysteresis loops exhibit at the end of the loading cycles a linear part which intercepts the origin of the stress-strain coordinate axes. This is a typical behavior of damageable elastic material. Nevertheless, some difference is apparent between the two types of composites. The curvature of the non-linear domain is lower and more smooth up to 0.2 % in strain for the C(B) composition graded interphase. Moreover, after being submitted to equivalent stresses, the samples with C(B) interphases exhibit residual strains 50 % higher and hysteresis loops areas 30 % higher than for their counterparts with PyC interphases. This difference suggests that the C(B) graded composition interphase leads to a slightly weaker fiber-matrix bond than the classical PyC interphase [8].

3.3. Oxidation resistance.

The 2D SiC/C(B)/SiC composites, submitted to ageing treatments in air under bending loading, exhibit lifetimes of 513-601 hrs at 500 °C, 22-43 hrs at 600 °C and 4-7 hrs at 700 °C. These values are of the same order as those obtained under similar conditions for the classical 2D SiC/PyC/SiC composites [9]. The improvement with respect to 2D-SiC/PyC/SiC composites previously obtained in an ageing study carried out on the corresponding microcomposites [4] could not be found again. This difference could be explained on the basis of the two main following reasons. The first may be related to the difference in the applied load pattern : tensile ageing at a stress close to

the proportional limit for the microcomposites and binding ageing at a stress largely higher than the proportional limit for the 2D-real composite. The second could be a difference between the microstructure of the C(B) graded composition interphase in the microcomposite (CVD process) and the 2D composite (CVI process), although the composition gradient is similar in both cases, as shown by the AES profiles [4].

3.4. TEM characterization of 2D SiC/C(B)/SiC composites

3.4.1. C(B) interphase in the composite

Figure 5 gives a bright field image of the C(B) interphase close to a transverse fiber (the thin foil presently studied is taken from a sample submitted to tensile test). Layers 1 and 2 are clearly apparent owing to a marked difference in contrast. The first appears as a uniform high grey, probably related to a poorly organized pyrocarbon. Conversely, the second exhibits (i) a columnar microstructure of the C(B) with a growth direction perpendicular to the fiber surface and (ii) a high crystallization state as shown by a dark grey contrast. The layers 3 and 4 are very similar with a high contrast, including dark zones (probably nanometric well-crystallized grains) embedded in bright zones, corresponding to amorphous parts and/or nanometric pores. Layer 5 is difficult to distinguish from the matrix, a feature which could result from a partial infiltration of SiC within this part of the interphase.

Figure 6 shows the EELS spectrum for each layer of the C(B) graded interphase. Carbon (K edge at 284 eV) and boron (K edge at 188 eV) are evidenced and the boron content increases from layer 1 to layer 4. In layer 5, a silicon peak ($L_{2,3}$ edge at 99 eV) is observed, which partially overlaps the boron peak. This last result seems to confirm the occurrence of some infiltration of SiC within the matrix side part of the interphase.

The very dark nanometric crystals (up to 20 nm in size) visible in the bright field image of layer 3 and 4 were analysed by microdiffraction (with a spot size of 10 nm), as shown in figure 7. The obtained pattern is quite surprisingly that of ß-SiC nanocrystals.

On the basis of all the observations reported above for layers 3 to 5, a nano-porous C(B) microtexture can be suggested, whose porosity is partially filled with SiC nanocrystals.

Further investigations on the various parts of this C(B) composition graded interphase were carried out by high resolution transmission electron microscopy (HRTEM). The image of layer 1 can be associated to a weakly organized pyrocarbon, with only a slight anisotropy (Fig. 8). This type of pyrocarbon is very similar to the one obtained under identical conditions by CVD for microcomposites [4]. Layer 2, shown in the lower part of the image in figure 9, exhibits a very high anisotropy with the carbon layer stack oriented parallel to the fiber axis. This layer is also very similar to the corresponding layer obtained by CVD in microcomposites [4]. Layers 3 (upper part of figure 9) and 4 (figure 10) reveal lattice fringes with marked contrasts and carbon layer stacks which form winding sheets (about 5 nm in width and up to 50 nm in length) without preferred orientation. At the interface between layer 2 and 3, stacks of layer 3 occur perpendicularly to stacks of layer 2. Between these sheets, weakly contrasted zones (about 10 nm in size) appear which could be either amorphous solid or crystals whose orientation do not fulfil the Bragg conditions or at last porosity. In the HRTEM image of layer 4 (Fig. 10), nanocrystals of ß-SiC (with (111) planes slightly visible) were evidenced as in bright field images (Fig. 7). The occurrence of such nanocrystals seems to confirm the presence of nano-porosity within layers 3 and 4. This sponge-like nanotexture is very different from the more dense nanotexture of corresponding interphase layers resulting from CVD in microcomposites [4].

3.4.2. C(B) interphase prior to matrix infiltration

In order to understand the effect of matrix infiltration on the nano-structure of the C(B) graded interphase in the 2D composites, the interphase was observed before infiltration using TEM. High magnification bright field image (Fig. 11) shows also a nano-porous microtexture for layers 3, 4 and 5, but these layers cannot be distinguished.

On the other and, layer 2 contains singular crystals similar to those observed in the corresponding layer of the C(B) interphase in microcomposites. Identical reticular distances are deduced from a selected area diffraction pattern recorded for these crystals (Fig. 12). (111) lattice fringes of this phase are visible in figure 13. This HRTEM observation shows that these crystals are mixed here with amorphous carbon due to Ar^+ ion milling effect.

Thus, the infiltration of the matrix in the 2D composites is not the cause of the sponge-like nanotexture of the boron-rich part of the C(B) graded interphase, the corresponding layers being slightly infiltrated by SiC. Conversely, the singular crystals, identified as diamond-like structure with many stacking faults in microcomposites [4], seem to have disappeared during the densification (i.e. at 1000 °C and during several hundreds hours), which is consistent with the metastable nature of the nanocrystals.

The nano-porous texture observed for layers 3, 4 and 5 could result from the stagnation of by-products (such as HCl) together with the reactive species within the fibrous preform. The growth rate of such boron-rich layers being very high [10], HCl and H_2 species could be confined inside the solid deposit, which could lead to the formation of partly open nano-pores. Consequently, SiC matrix could be infiltrated within such layers.

3.4.3. Localization of the matrix cracks deviations

As shown in figure 14, the tensile test results in deflection of the matrix cracks and their propagation mostly within layer 2, i.e. the most organized layer. The nano-porous part of the interphase (layers 3 to 5) does not deviate the crack. Layer 2 seems to be responsible for the good ambient mechanical properties of the composite. This feature is consistent with the assumption that matrix crack deflection is favored in interphase displaying a layered crystal structure or a layered microstructure [11]. Figure 15 shows another crack deflection which occurs between layer 2 and 3 as in microcomposites [6].

3.4.4. C(B) interphase after ageing test

To try to explain the relatively weaker behavior of the present 2D SiC/C(B)/SiC composites when submitted to an ageing treatment in air under load, the C(B) graded composition interphase was observed by TEM after such a test.

TEM bright field observations have shown that only the interphases deposited on transverse fibers (i.e. perpendicular to the sample axis) have been oxidized. This result can be explained by (i) the shorter path way for oxygen along these fibers than along the longitudinal fibers and (ii) the localization of the matrix cracks in the plane of transverse fibers, the corresponding interphases being more rapidly exposed to air.

Bright field image in figure 16 shows a zone of the interphase where it has been partially oxidized. Layers 1, 3, 4 and 5 were replaced by an amorphous material (its electronic diffraction pattern is a diffuse halo) which seems to contain bubbles being possibly entrapped in the sample during cooling. EELS analysis shows that this material is mainly made of silica, as for the oxidized interphase in microcomposites. Layer 2 in the present 2D composite seems to have better resisted to oxidation for it was only partially replaced by silica, as shown in the EELS spectrum of figure 17. The more rapid consumption of layer 1 can be attributed to the absence of boron on the one hand, whereas that of layers 3, 4 and 5 can be assigned to their porous nanotexture which gives them a high specific surface exposed to air on the other hand. Finally, figure 18 shows another region of the oxidized interphase where all the layers are replaced by silica, as confirmed by EELS analysis.

In the various samples observed by TEM after ageing, the absence of boron in the oxidized interphases could be explained by the extreme reactivity of boron oxide towards water vapor of air, giving rise to boric acid which is highly volatile even at ambient temperature [12]. This phenomenon could be enhanced during the thin foils preparation.

4. Conclusion

2D SiC/SiC composites with a composition graded C(B) interphase made of five layers (with a boron content increasing from the fiber to the matrix) were prepared by CVI. This interphase results in ambient mechanical characteristics of the 2D composites similar to those of the corresponding material with a pure pyrocarbon interphase. Conversely, it seems not to favor an increase in the lifetime of such composites when submitted to thermal ageing in air under load, while a similar interphase has been reported [4] to increase the lifetime of their microcomposite counterparts.

By TEM characterization, the two first layers close to the fiber (pure pyrocarbon and 8 at. % boron C(B) material) were found to be very similar to those obtained by CVD in microcomposites. The layer 2 is a highly organized turbostratic boron doped carbon. The diamond-like nano-crystals observed in microcomposites [4] seam to have disappeared during the CVI process of SiC matrix. On the contrary, the layers close to the matrix (layers 3, 4 and 5) exhibit a texture highly different from those in the microcomposites which displays a sponge-like aspect with numerous nano-pores. This internal porosity could explain the low lifetime observed for these composites owing to a rapid diffusion of oxygen within such layers.

A better control of the growth process of the boron-rich layers in the interphase infiltration in order to obtain dense films, could improve the lifetime of the real composites and lead to a behavior similar to that previously reported for the microcomposites.

ACKNOWLEDGEMENTS

This work has been supported by CNRS and SEP through a grant to S. J. The authors wish to thank SEP for mechanical and ageing tests and are grateful to F. Doux from SEP, X. Bourrat and H. Tenailleau from LCTS, and M. Lahaye from CUMENSE for fruitful discussion.

REFERENCES

[1] R. Naslain, "Fiber-matrix interphases and interfaces in ceramic-matrix composites processed by CVI", Composite Interfaces, 1 [N° 3], pp 253-286, (1993).

[2] A.G. Evans and F.W. Zok, "The physics and mechanics of fibre-reinforced brittle matrix composites", J. Mater. Sci., 29, pp 3857-3896, (1994).

[3] J.M. Jouin, J. Cotteret and F. Christin, "SiC/SiC interphase : case history", Proc. 2nd European Colloquium "Designing Ceramic Interfaces" CEE Joint Research Centre, Petten (NL), Nov. 11-13, (1991).

[4] S. Jacques, A. Guette, F. Langlais, R. Naslain, "C(B) materials as interphases in SiC/SiC model microcomposites", in PhD Thesis N° 1398, Univ. Bordeaux I (France), (1995), to be published.

[5] R. Naslain, J.Y. Rossignol, P. Hagenmuller, F. Christin, L. Heraud and J.J. Choury, Rev. de Chim. Min.,18, p 544, (1981).

[6] S. Jacques, A. Guette, F. Langlais and X. Bourrat, "Characterization of SiC/C(B)/SiC microcomposites by transmission electron microscopy", in PhD Thesis N° 1398, Univ. Bordeaux I (France), (1995), to be published.

[7] L. Guillaumat, "Microfissuration des CMC : relation avec la microstructure et le comportement mécanique", PhD Thesis N° 1056, Univ. Bordeaux I (France), (1994).

[8] C. Droillard, J. Lamon and X. Bourrat, "Strong Interface in CMCs, Condition for Efficient Multilayered Interphases", Mat. Res. Soc. Symp. Proc., R.A. Lowden, J.R. Hellmann, M.K. Ferber, S.G. Di Pietro and K.K. Chawla eds., Nov. 1994, Materials Research Society, Vol. 365, pp 371-376, (1995).

[9] SEP private communication.

[10] S. Jacques, A. Guette, X. Bourrat, F. Langlais, R. Naslain, C. Guimon and C. Labrugère, "LPCVD and characterization of boron-containing pyrocarbon materials", in PhD Thesis N° 1398, Univ. Bordeaux I (France), (1995), to be published.

[11] R. Naslain, "The concept of layered interphases in SiC/SiC", A.G. Evans and R. Naslain, eds, Ceram Trans, vol. 58, pp. 23-39, The Amer. Ceram. Soc., Westerville (OH), USA, 1995.

[12] K. Kobayashi, K. Maeda, H. Sano and Y. Uchiyama, "Formation and oxidation resistance of the coating formed on carbon material composed of B_4C–SiC powders", Carbon, 33 [N° 4], pp 397-403, (1995).

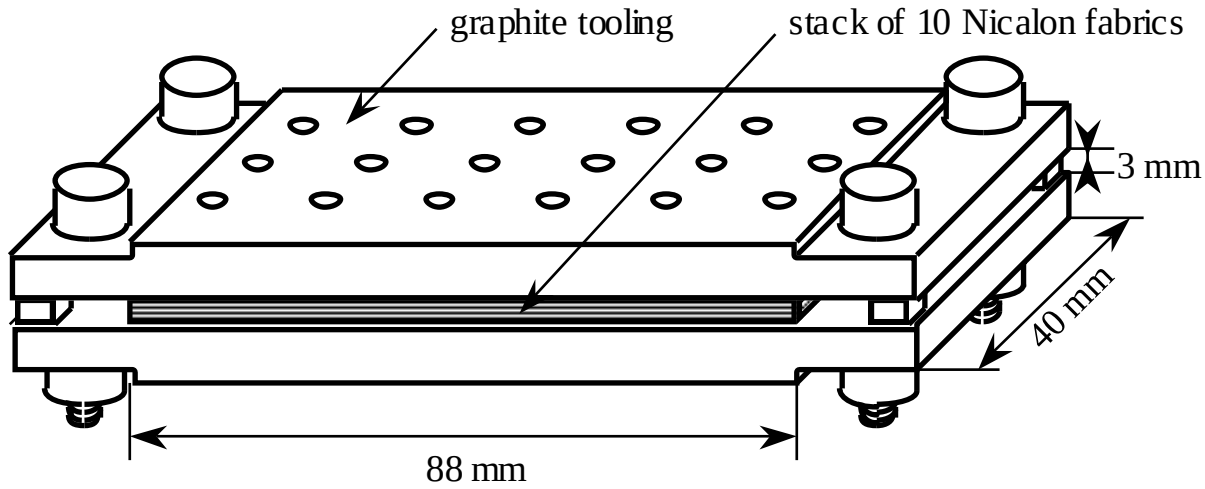

Fig. 1: Graphite tooling in which the stack of Nicalon fabrics is maintained during the CVI process of C(B) interphase (Schematic).

α (%)	layer	infiltration time (min)	mean thickness (nm)
0	1	240	~ 80
30	2	8.3	~ 80
50	3	7	~ 80
70	4	18	~ 80
85	5	30	~ 80

Table I: Infiltration durations and thicknesses of C(B) interphase layers as a function of the initial gas phase ratio a = 100 x **Erreur !**where Q(i) stands for the gas flow rate of species i under standard conditions.

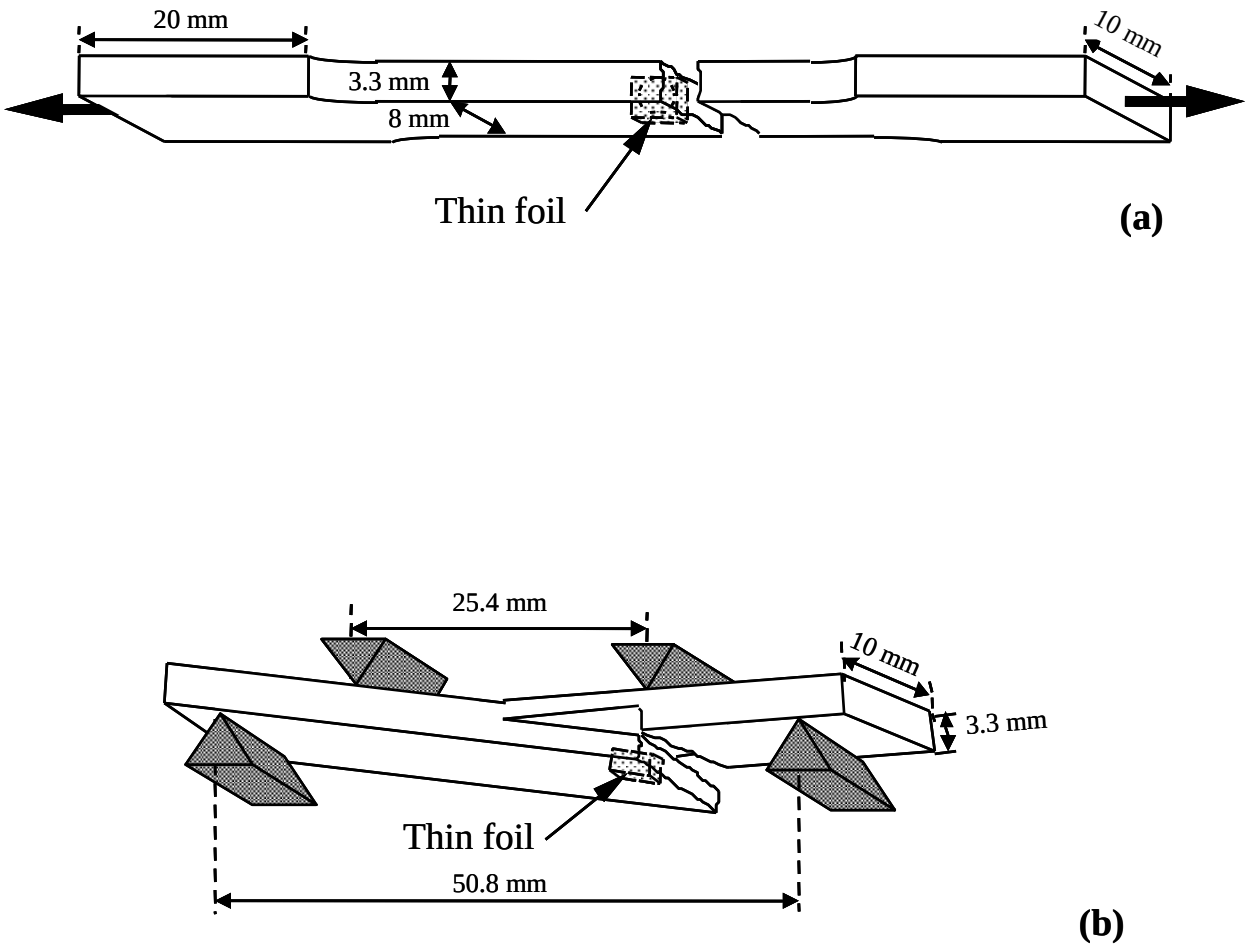

Fig. 2: Location of the thin foil sample after failure in the tensile test specimen (a) and in the bending test specimen (b).

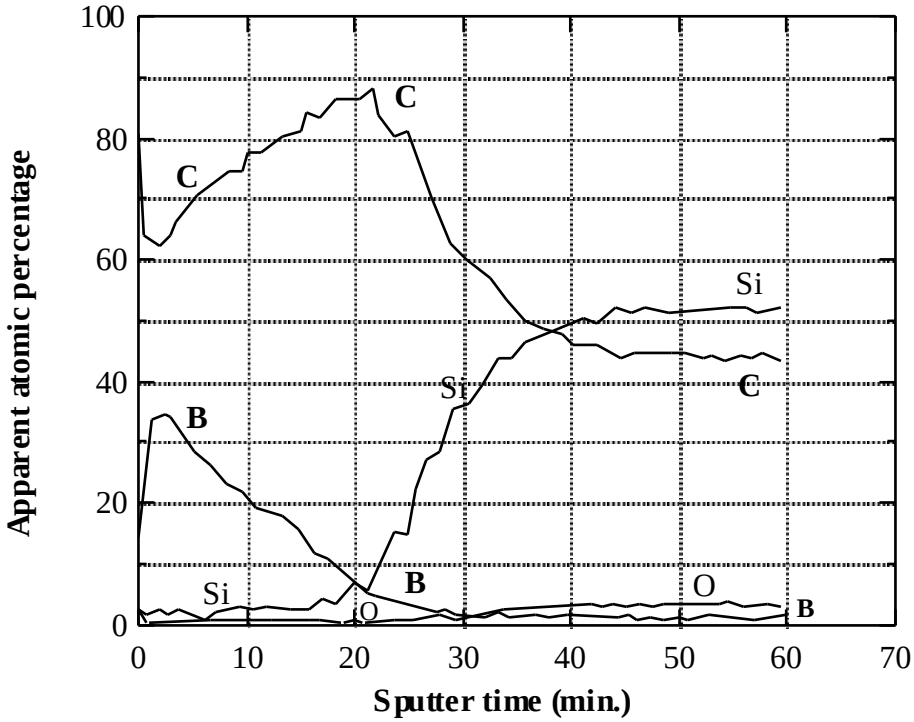

(a)

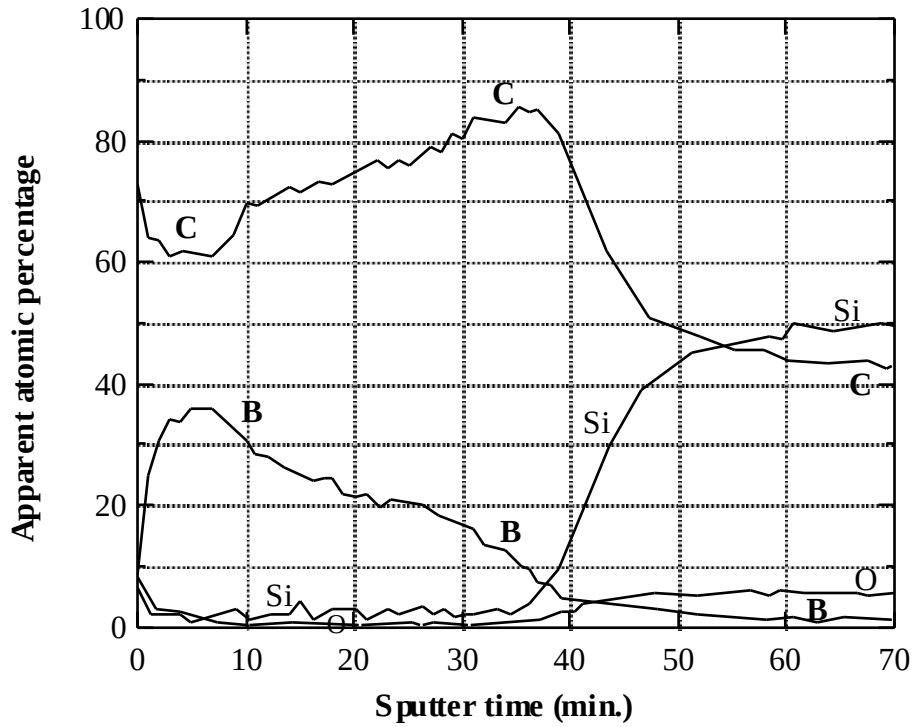

(b)

Fig. 3: AES depth atomic concentration profiles for the C(B) composition gradient interphase in the center (a) and on the periphery (b) of the fibrous preform prior to matrix infiltration.
(Sputter rate: 20 nm/min ; ref. Ta_2O_5)

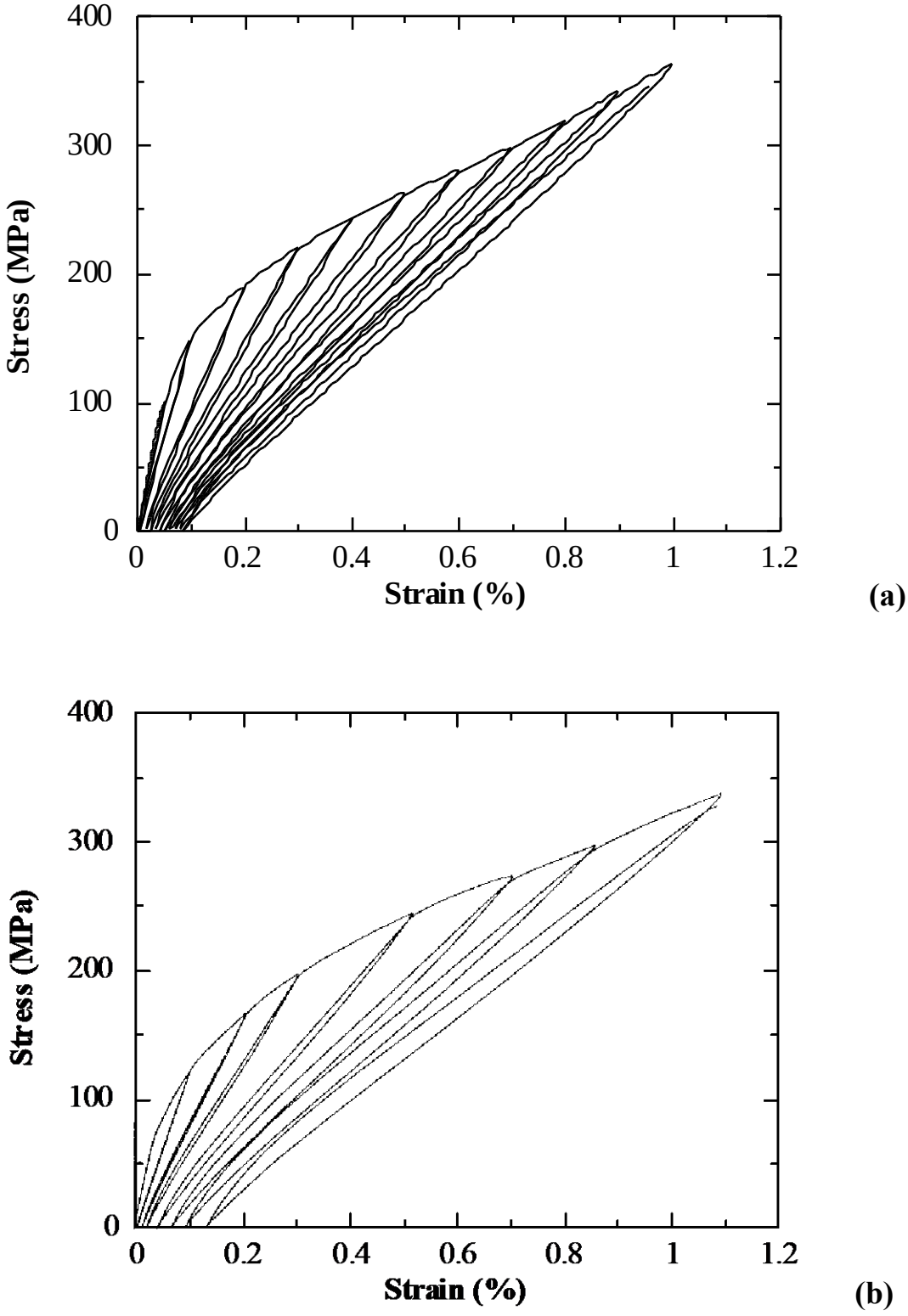

Figure 4: Tensile stress-strain curves with load cycles for (a) 2D SiC/PyC/SiC and (b) 2D SiC/compositional gradient C(B)/SiC.

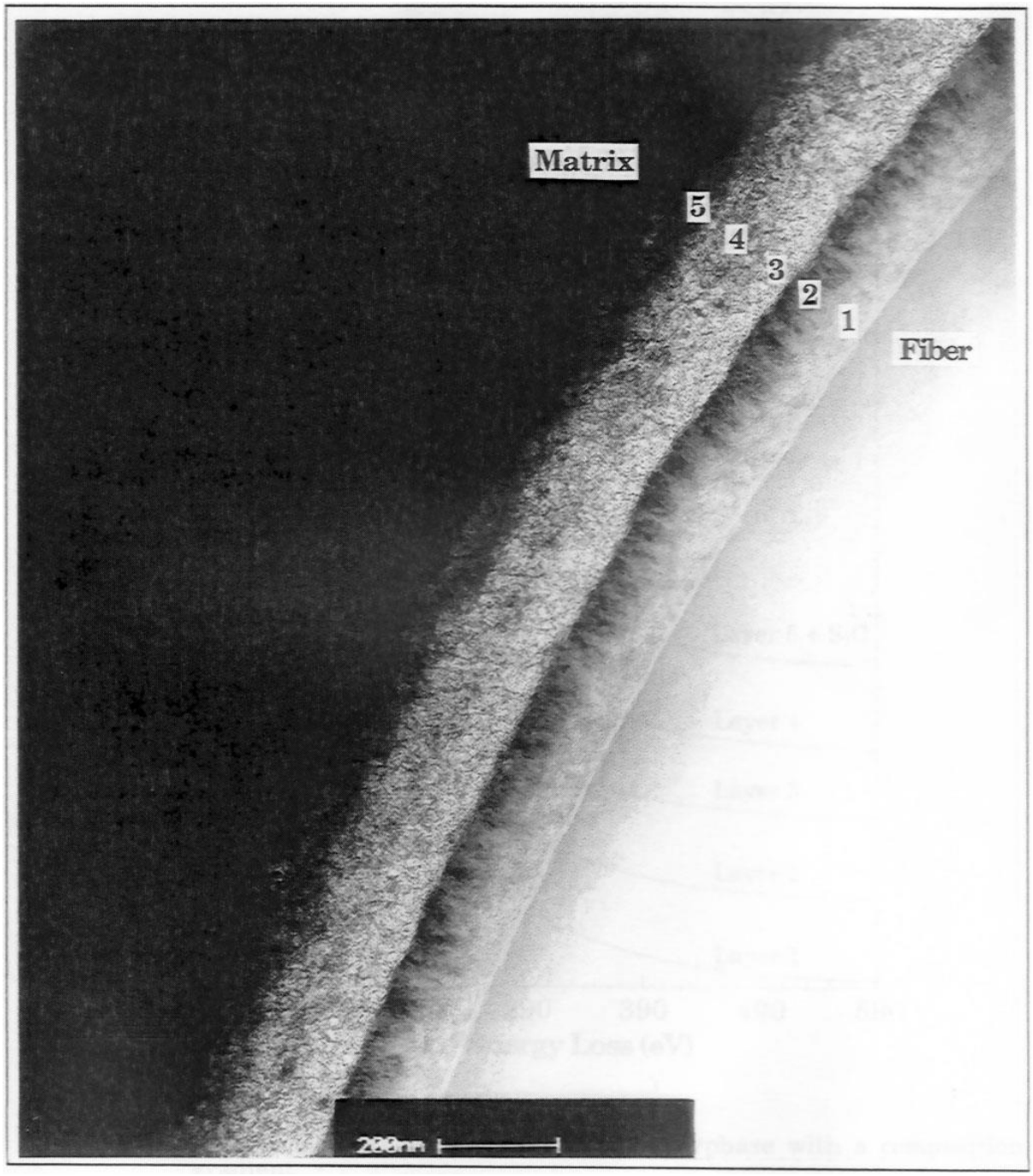

Figure 5: Bright-field TEM image of the composition graded C(B) interphase showing the five interphase layers.

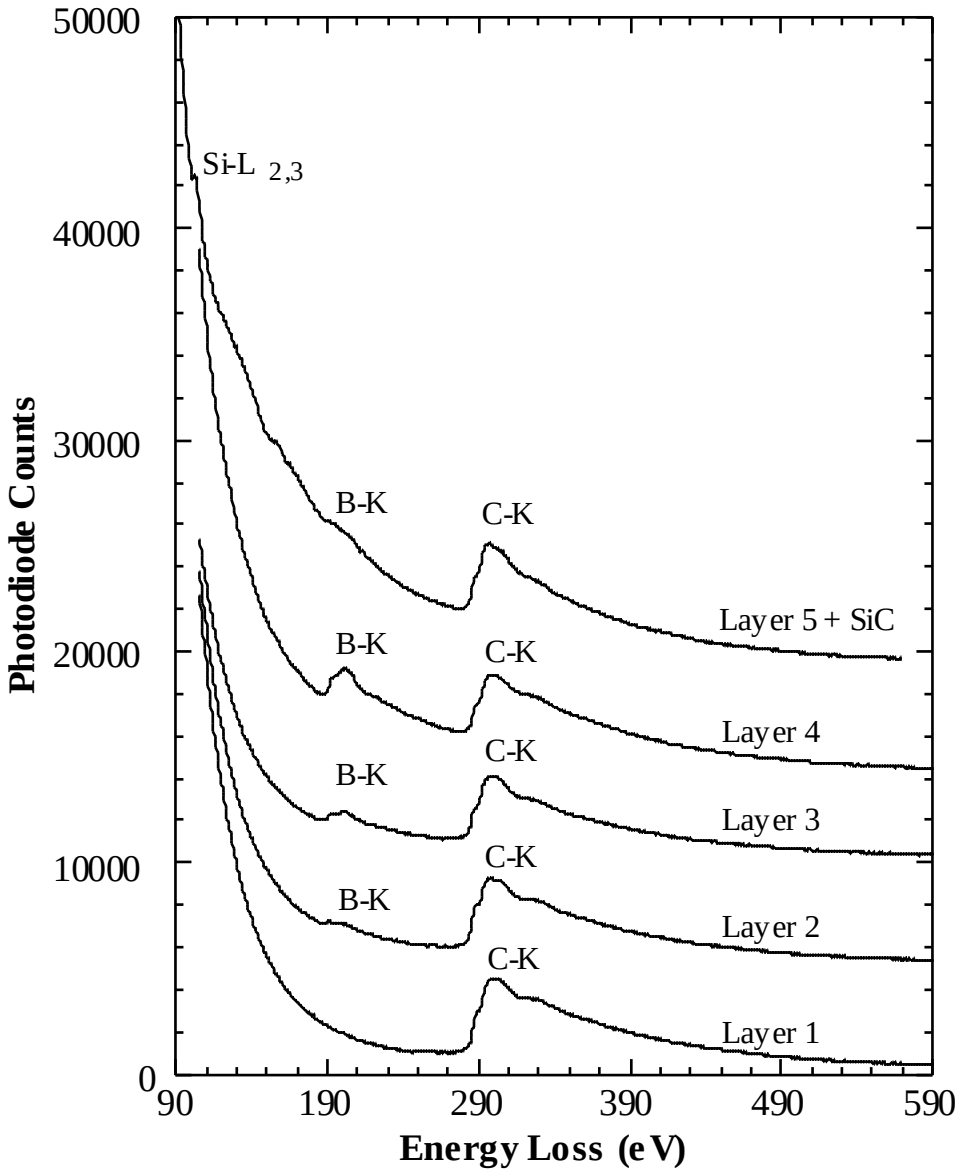

Fig. 6: EELS spectrum from the CVI C(B) interphase with a composition gradient.

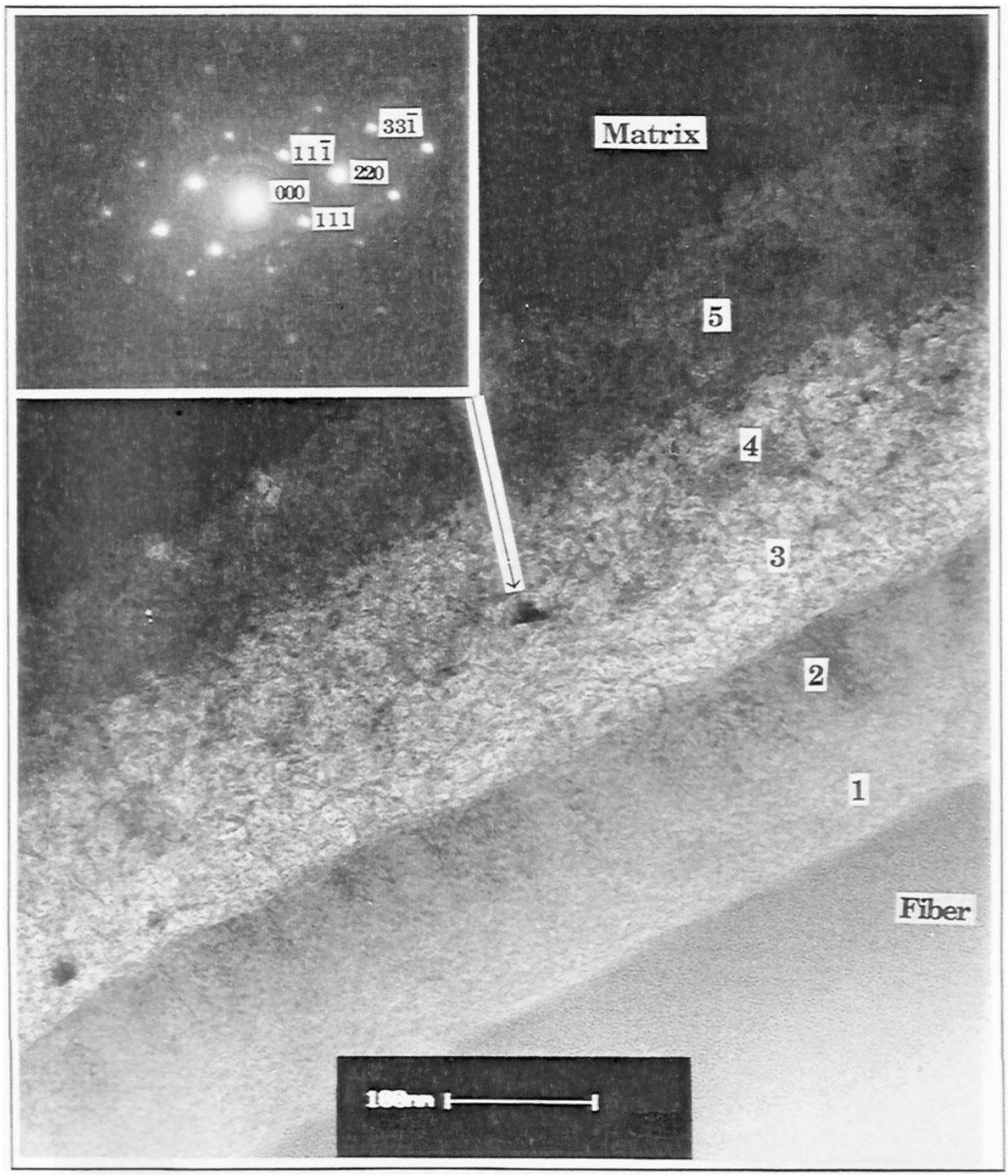

Figure 7: Bright-field TEM image of the interphase with microdiffraction (insert) of a nano-crystal entrapped in layer 4.

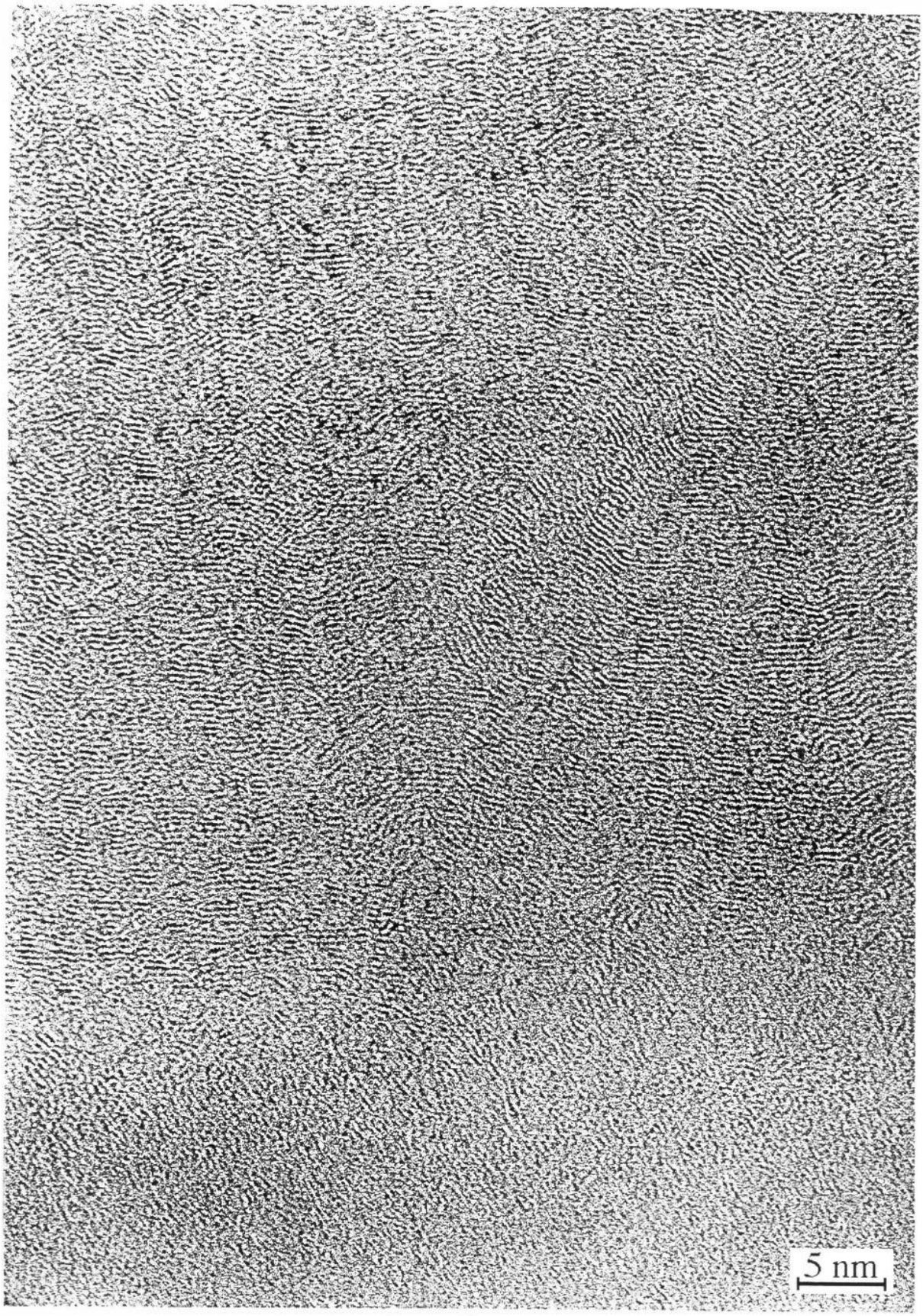

Figure 8: HRTEM image of layer 1.

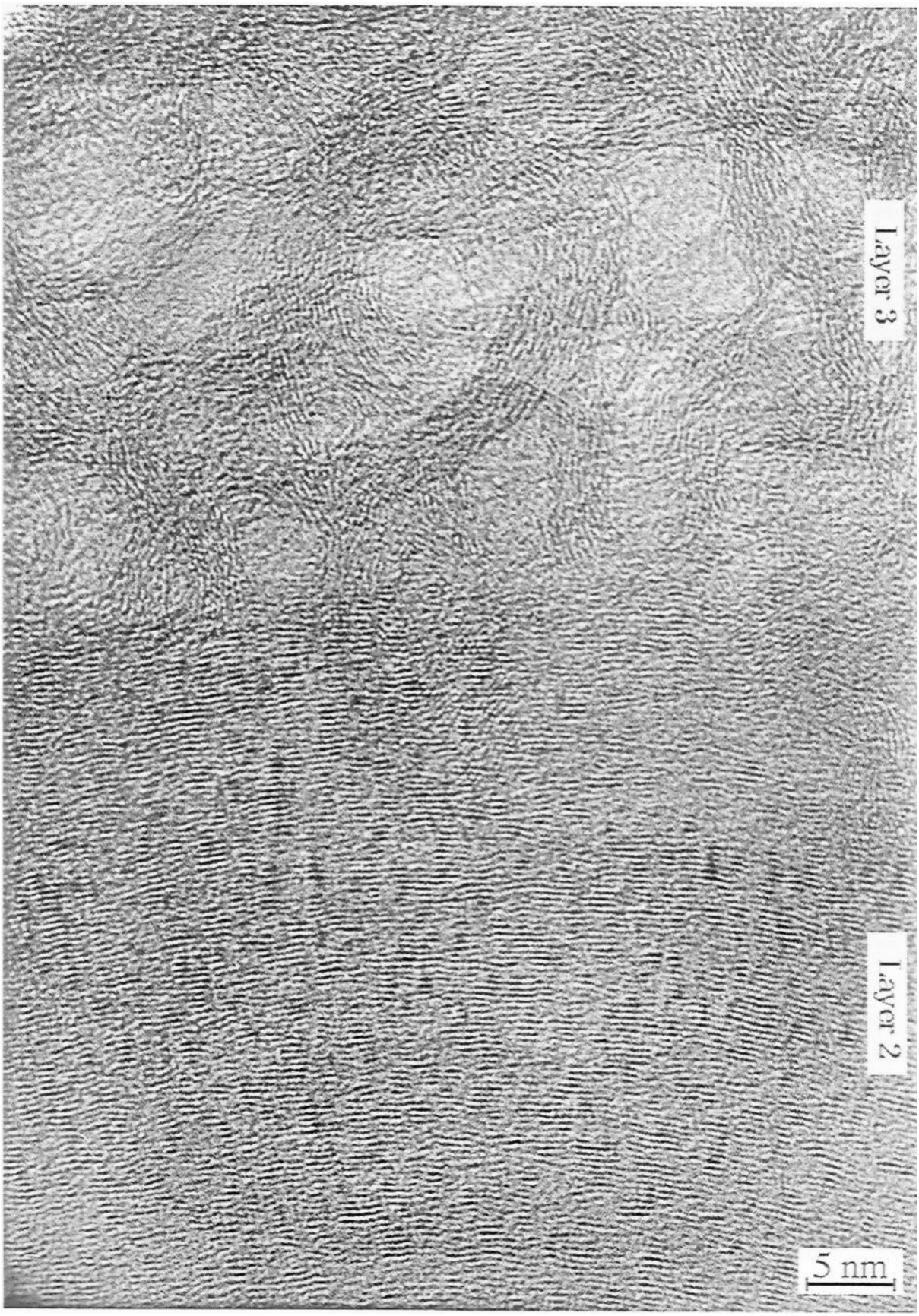

Figure 9: HRTEM image of layers 2 and 3.

Figure 10: HRTEM image of layer 4.

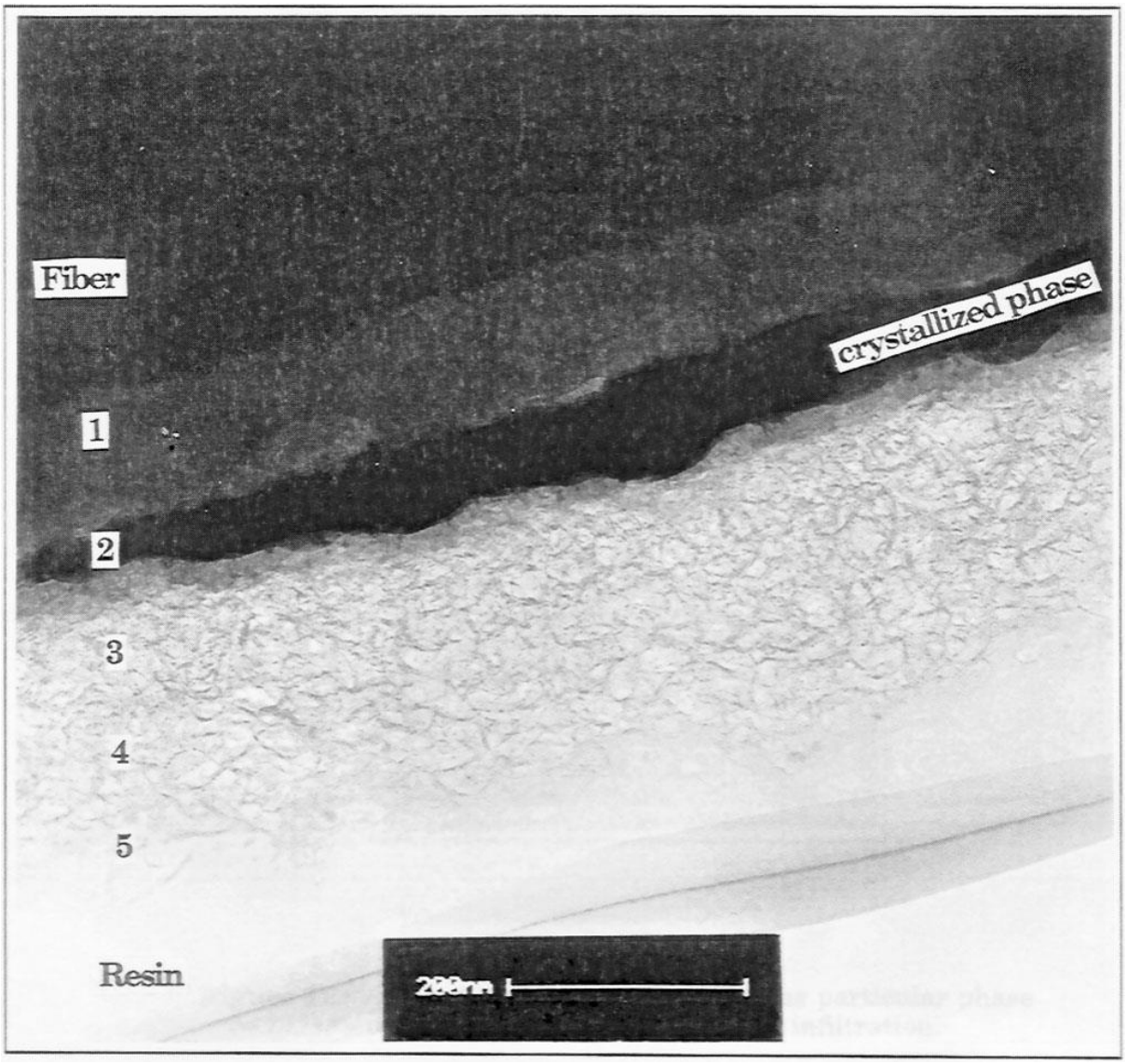

Figure 11: Bright-field TEM image of the interphase prior to matrix infiltration.

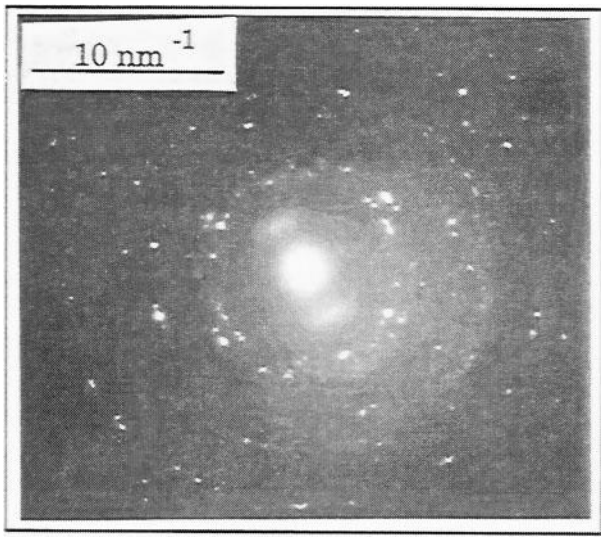

Figure 12: An electron SAD pattern from the particular phase present in layer 2 prior to matrix infiltration.

Figure 13: HRTEM image of the particular phase present in layer 2 prior to matrix infiltration.

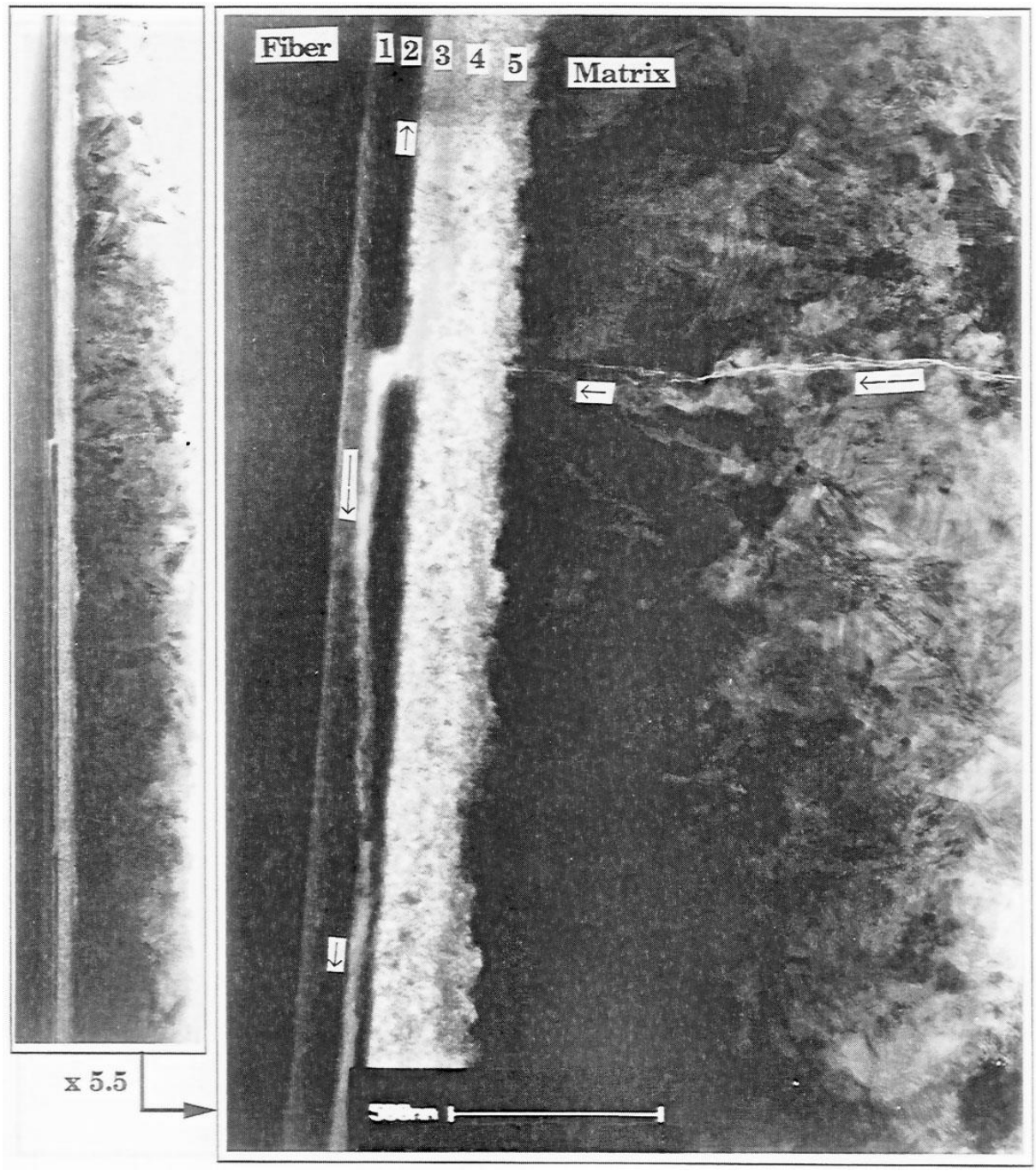

Figure 14: Bright-field TEM images of a matrix crack deflection in the composition graded C(B) interphase.

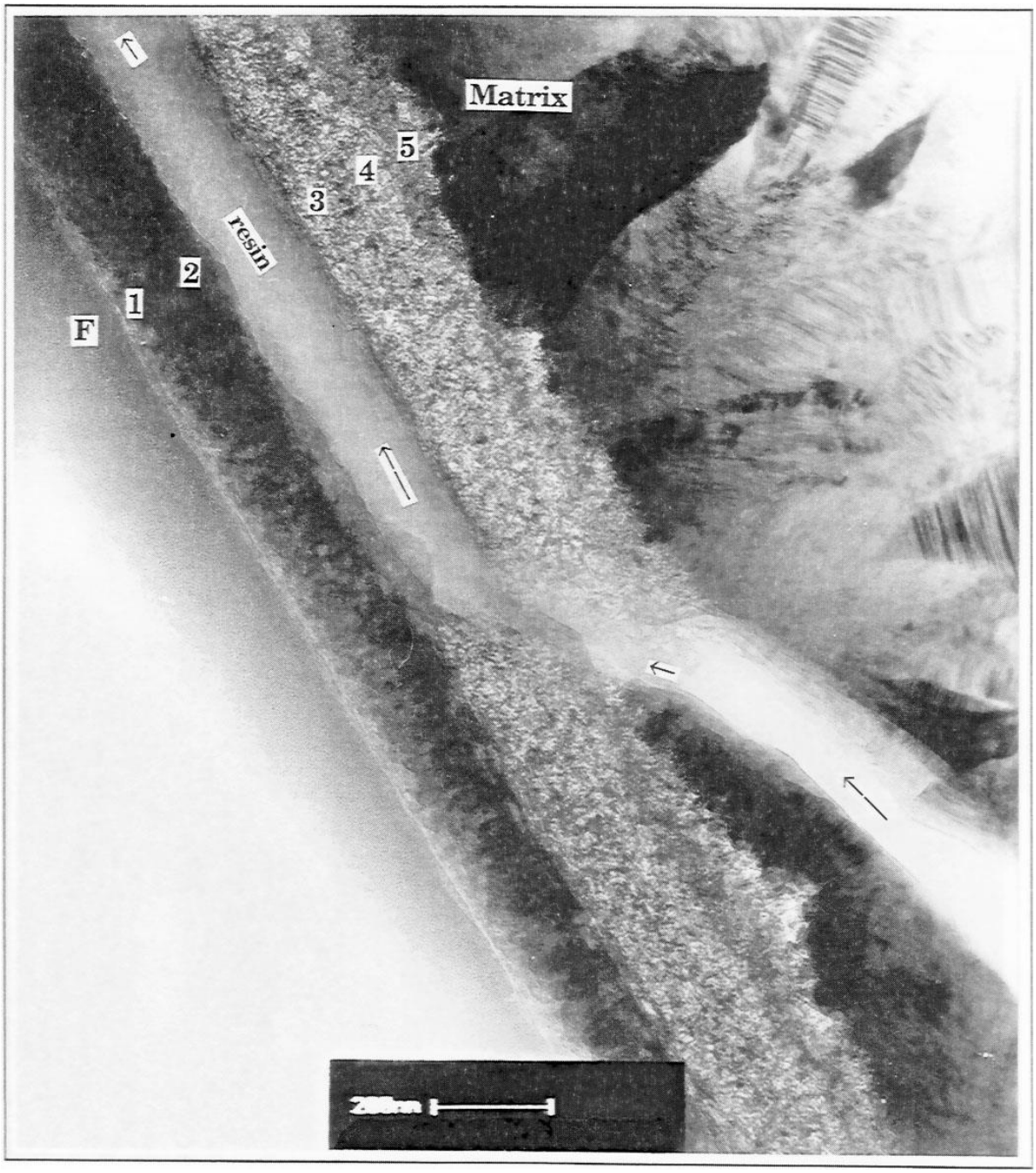

Figure 15: Bright-field TEM image of a matrix crack deflection in the composition graded C(B) interphase.

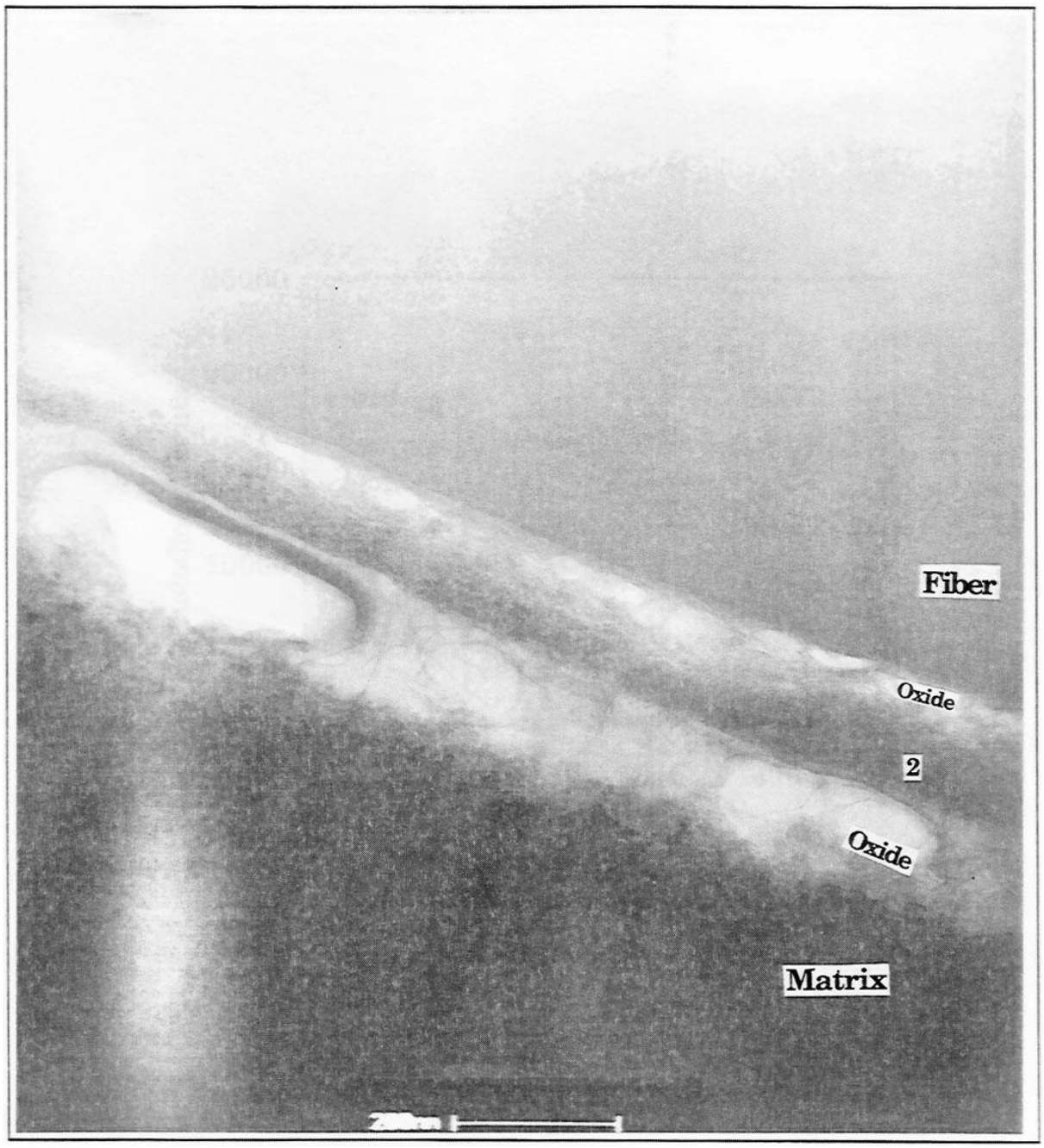

Figure 16: Bright-field TEM image of the partially oxidized composition graded C(B) interphase.

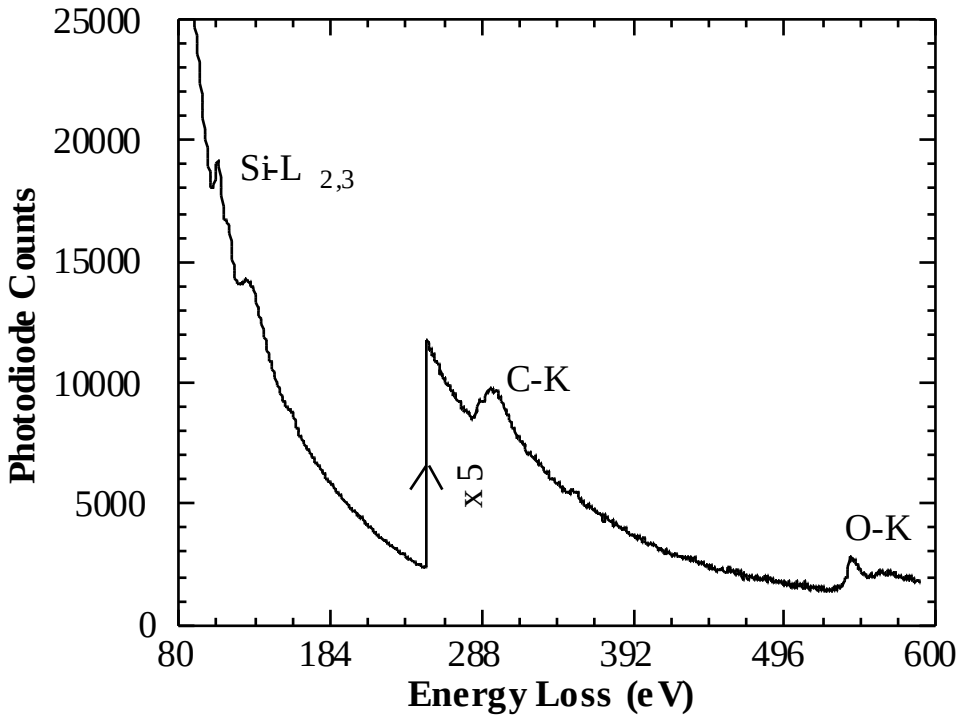

Fig. 17: EELS spectrum from the partially oxidized layer 2 .

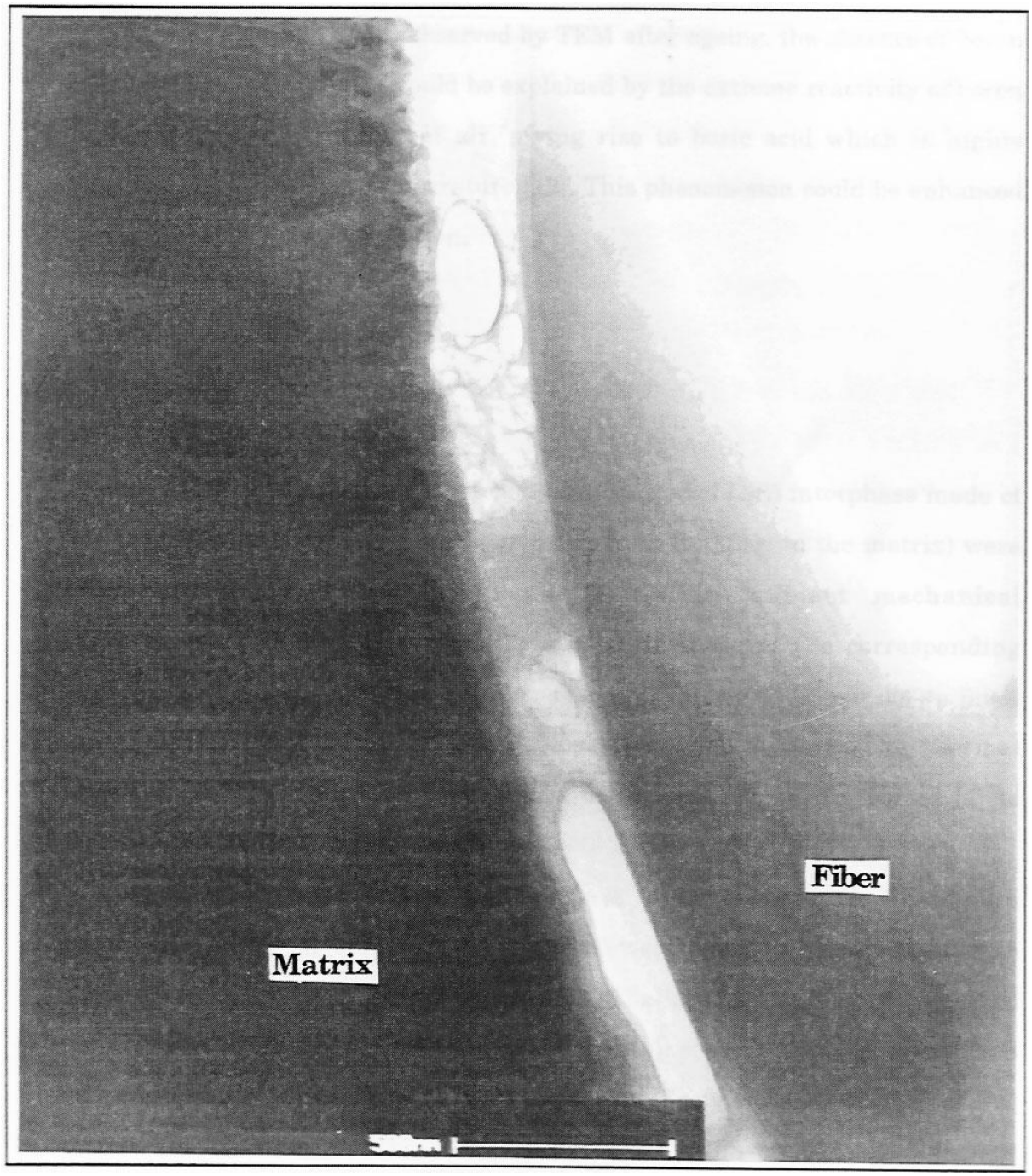

Figure 18: Bright-field TEM image of the oxidized composition graded C(B) interphase.